

## Extension of Pocket Machining to Direct Write Lithography

Manseung Seo<sup>1</sup> and Haeryung Kim<sup>2</sup>

<sup>1</sup>Tongmyong University, [sms@tu.ac.kr](mailto:sms@tu.ac.kr)

<sup>2</sup>Tongmyong University, [hrkim@tu.ac.kr](mailto:hrkim@tu.ac.kr)

### ABSTRACT

A lithographic path generation method for direct write lithography is devised by adopting the offset curve and tool path generation method in pocket machining. In lithography, unlike machining, overlapping of the tool trajectory results in the accumulation of the light beams' energy. The difference between the offset in machining and the lithographic offset is analyzed. The role of the lithographic tool is essentially established for the beam. A sheaf of laser beams is considered as a lithographic tool instead of a single to obtain smoothed and flattened distribution of irradiance. Moreover, over milling and tool retraction are reconsidered in the view of energy accumulation and isolation. The accuracy of the method is ensured by the uniformity of the irradiance. The efficiency of the method is increased upon the shortening of the lithographic path. The implementation results verify that our strategy of extending pocket machining to direct write lithography is proper and reliable.

**Keywords:** Maskless Lithography, Direct Write Lithography, Pocket Machining.

### 1. INTRODUCTION

Conventional lithography using masks has been the workhorse in the field since it was invented in the 18th century. Even now, most of the lithography carried out use masks. Due to the problems caused by masks such as expense and time in fabricating the masks, contamination by masks, disposal of masks, and the alignment of masks, research of maskless lithography was initiated recently and it is growing rapidly and broadly.

Recently, devices using micromirror arrays such as the Digital Micromirror Device (DMD) by Texas Instruments Inc. (TI) and the Spatial Light Modulator (SLM) have brought innovation to the field of microdisplays. The DMD and SLM are considered as the successful solution to digital light processing and Micro Electronic Mechanical System (MEMS). Nowadays, many new application fields for them have emerged, and one of them is maskless lithography [1-3]. However, this is feasible if, and only if, each system developer could set up an excellent optic unit, and an accurate lithographic pattern generation system to control millions of micromirrors individually and instantaneously.

On the other hand, direct write lithography has long been applied to photomask fabrications using a laser in the field of microelectronics and extended to nanosize fabrications using an electron beam [4-6]. However, these may neither be sufficient in throughput nor be efficient in time. Some may not be appropriate for mass production because of time consumption in controlling the beam for on/off or in varying the size of aperture for irradiation while in fabrication. One with a zigzag path may not be proper to apply for the fabrication of a large lithographic extent.

In this study, we focus on the process time of direct write lithography especially for large lithographic extent. Upon our familiarity and preliminary works on maskless lithography using micromirrors [3] and pocket machining [7], the extension of pocket machining to direct write lithography is initiated.

As the first step of extension, we aim to derive a method of direct write lithographic path generation by adopting the offset curve generation method and tool path generation method. For the adoption of the Offset-loop Dissection Method (ODM) [7], the difference between the offset in machining and lithographic offset is analyzed in the view of energy accumulation. To obtain uniform exposure intensity throughout the whole extent of the pattern for high lithographic quality, the role of the lithographic tool is essentially established for the beam. For the adoption of the Path Determination Method (PDM) [7], over milling and tool retraction are reconsidered in the view of energy accumulation and isolation. The characteristics of the lithographic path are applied to reduce lithography time and to achieve even exposure intensity.

For verification, a prototype system is implemented and examined with actual display patterns, which are the barrier rib of the Red, Green and Blue (RGB) pattern and the Indium Tin Oxide (ITO) pattern. The results verify that the proposed approach is proper and reliable.

The devised direct write lithographic path generation method is concise and simple, but robust and flexible enough to generate a lithographic path under constraints such as energy accumulation, isolation and consumption. Moreover, the accuracy of the method is proved by the uniformity of the exposure intensity throughout the whole extent of the pattern and the efficiency of the method is increased upon the shortening of the lithographic path.

## 2. DERERMINATION OF LITHOGRAPHIC OFFSET

The critical difference between pocket machining and direct write lithography comes from the accumulation of energy. In lithography, overlapping of the lithographic tool trajectory results in the accumulation of the light beams' energy, i.e., overlay intensity, which significantly affects the lithographic quality when it is not even. Therefore, the selection of the tool for direct write lithography needs to be performed based on its spatial characteristics such as exposure intensity profile or irradiance distribution and the determination of the lithographic offset must be accomplished considering the overlap of the overlaid intensity.

In the present study, we assume that the tool for direct write lithography is a laser operated in the fundamental Transverse Electromagnetic Mode (TEM). By choosing the laser beam in the theoretical TEM00 mode as the tool, the spatial distribution of the irradiance of the beam is fixed to be the ideal Gaussian in its intensity profile, even though the output from real life lasers is not truly normal. The TEM00 is known as the mode that is best collimated and produces the smallest spot of high power density for drilling, welding, and cutting.

However, in direct write lithography, it is quite inappropriate to use a laser beam with the Gaussian irradiance distribution having the smallest spot. The bell shaped profile of the laser beam causes an uneven irradiance distribution over the transverse of the lithographic offset, unless the lithographic offset is made the same as the spot size. To overcome the problem caused by the uneven irradiance using a laser beam, we devise a way of smoothing and flattening the top of the bell shaped irradiance distribution by considering a sheaf of laser beams as a lithographic tool.

Figure 1(a) shows the three-dimensional irradiance distribution of a single TEM00 laser beam. The two dimensional transverse intensity profiles of six overlapping TEM00 laser beams located along the  $r^*$  axis by a distance that is 16.67% of the diameter of a laser beam are shown in Fig 1(b) as dotted lines. The two dimensional transverse intensity profile obtained by the accumulation of six overlapping TEM00 laser beams is shown in Fig 1(b) as a solid line, and the three dimensional irradiance distribution of it is shown in Fig 1(c).

In comparison with the bell shape of the each intensity profile, the top portion of the accumulated intensity profile is much more flattened. If the other six are added next to the one shown in Fig.1(b) along the  $r^*$  axis by the same distance, the flattened length should be increased, and the more added then the flatter it becomes. Thus, it is confirmed that the approach to obtain even distribution of irradiance by considering a sheaf of laser beams as a lithographic tool is proper and reliable.

Especially for the fabrication of a large lithographic extent, the specification of a sheaf of laser beams and each beam in a sheaf increasing the flattened length may be needed. In TEM00 mode, the beam emitted from a laser begins as a perfect plane wave with a Gaussian transverse irradiance distribution. The, intensity profile  $I(r)$  may be written as:

$$I(r) = \frac{2P_o}{\pi\omega^2} e^{-2\frac{r^2}{\omega^2}} \quad (1)$$

Where,  $P_o$  is the total output power that is considered to be constant,  $r$  is the distance from the center of the bell shaped profile, and  $\omega$  is the radius of the laser beam in the common definition accepted for optics where the intensity,  $I(r)$ , falls to  $1/e^2$  which is 13.5% of the maximum intensity  $I_{MAX} = 2P_o / \pi\omega^2$  obtained at the axis of symmetry.

However, the common definition of the radius of the laser beam is not appropriate in this study, since we are dealing with an accumulation of irradiance. Neglecting 13.5% of the irradiance in lithography may fall in conflict. The radius should be determined upon laser specifications and lithography process conditions such as the removed away ratio of the Photo Resistant (PR) material through developing and/or the etched away ratio. To increase the flexibility, Eqn.1 may be rewritten in terms of dimensionless variables for scaling of the percentile intensity upon its minimum to maximum and the extended radius of a laser beam using one scaling parameter,  $S$ , as:

$$I^*(r) = \left( \frac{S}{e^2} \right)^{r^*2} \quad (2)$$

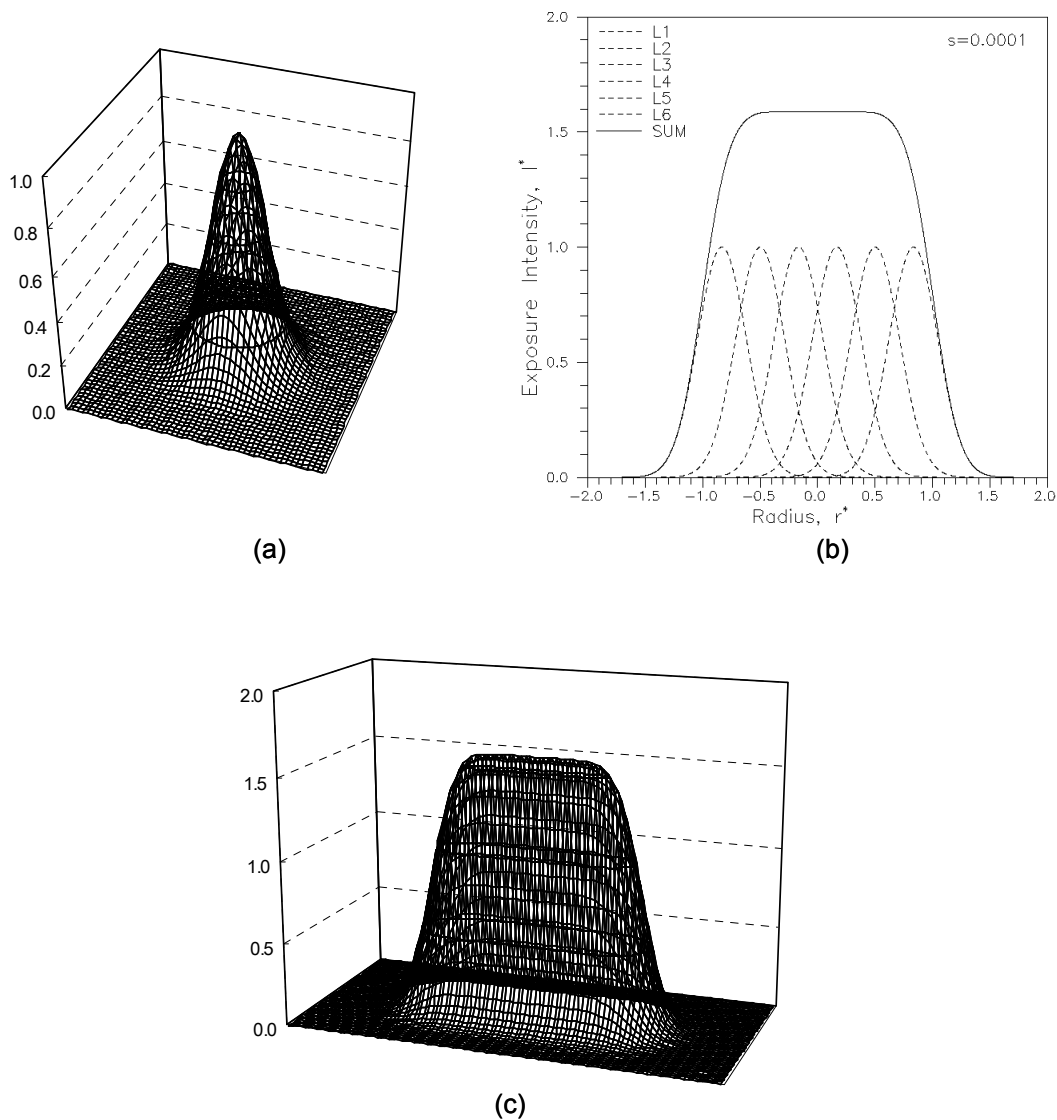


Fig. 1. Irradiance distribution of TEM00 laser beams.

Where,  $I^* = I / I_{MAX}$  and  $r^* = r / R$  with the extended radius of a laser beam defined as  $R = \omega \sqrt{1 - \ln \sqrt{s}}$ , so that the maximum dimensionless intensity  $I_{MAX}^*$  at  $r^* = 0$  equals 1 and the minimum dimensionless intensity  $I_{MIN}^*$  at  $r^* = 1$  equals  $s / e^2$ .

Figure 2 shows the irradiance distribution obtained by the accumulation of overlay intensity due to overlapping of one to seven laser beams at various assigned scaling factors ( $s$ ). The scaling factors for Fig.2(a), Fig.2(b), Fig.2(c), Fig.2(d), Fig.2(e), and Fig.2(f) are assigned as 1.0, 0.3, 0.05, 0.01, 0.001, and 0.000001, respectively, to obtain the most successive flattened intensity profile by the overlapping of 2, 3, 4, 5, 6, and 7 laser beams, respectively. The number of overlapping laser beams participating in overlapping as a set is  $N$  appearing in Fig.2 as  $NX$ , and each laser beam in a sheaf is located along the  $r^*$  axis by a distance that is  $(100/N)\%$  of the diameter of a laser beam.

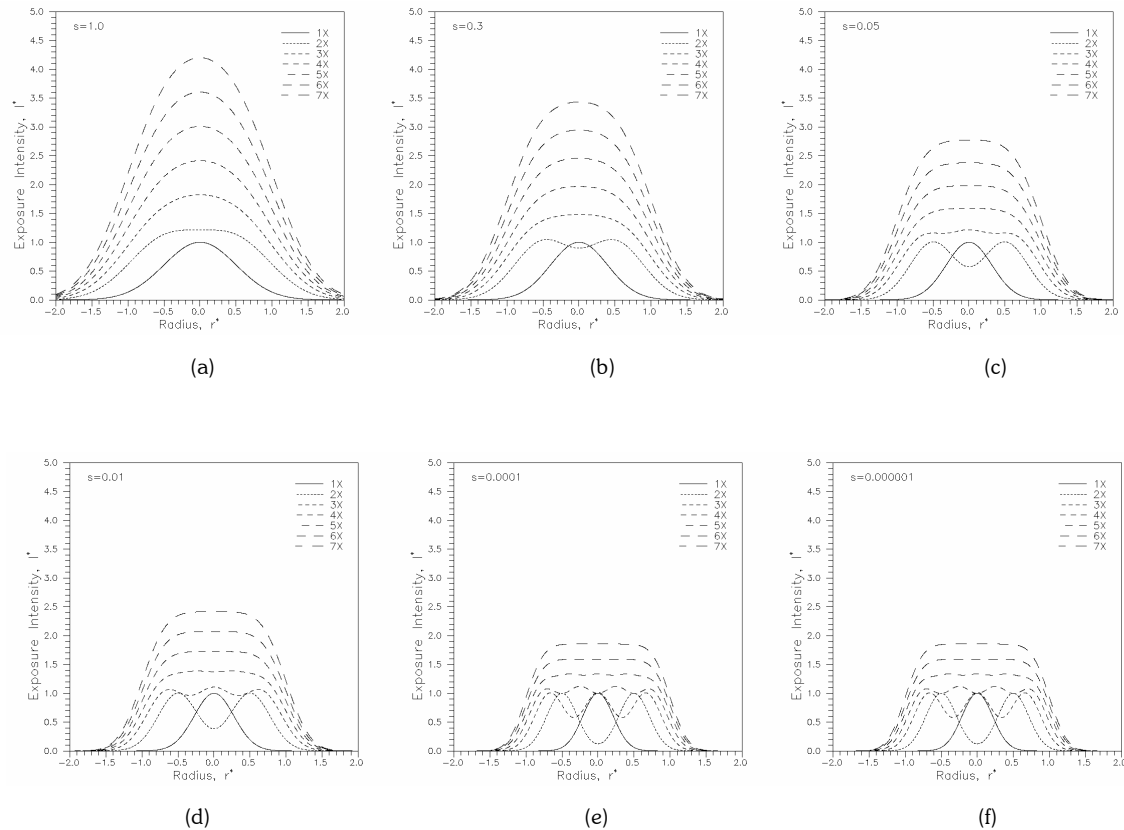


Fig. 2. Irradiance distribution at various scaling factor.

The flattened intensity profiles shown in Fig.2 insist that the extension of pocket machining to direct write lithography is feasible through this study. The lithographic quality through even distribution of irradiance is ensured in the proposed method, with the proper selection of the laser beam by referencing Fig.2, and with the accurate determination of the lithographic offset as  $(100/N)\%$  of the diameter of a laser beam when a sheaf of  $N$  overlapping laser beams plays the role of lithographic tool.

The thickness of the line drawn by a sheaf of  $N$  overlapping laser beams is examined. Table 1 shows half of the line thickness obtained at 50% of the maximum exposure intensity by considering that 50% of the PR is removed through developing and etching. Except the case using a single laser beam, most of the lines drawn by a sheaf of multi overlapping laser beams appear to have half the line thickness close to 1.0. The line thickness is conserved with 1% tolerance for the sheaves which result in the successive flattened intensity profile, written in bold italic letters in Tab.1. Through the devised method, the line center and the line thickness are always conserved.

On the other hand, there may be regions where the even irradiance from a sheaf of laser beams falls into conflict. The deviation from flattened irradiance distribution is expected on corners and irregular regions where extraordinary overlapping of offsets occur due to the trimming and merging of offset segments. The degree of imperfection to appear on a final product depends upon lithographic pattern geometries, lithographic speed variations, and lithography conditions such as PR removal ratio through developing and/or etching. Methods to compensate for deviation from the target irradiance due to irregular pattern geometry may be enumerated as specific adjustments of offset segments, redesign of pattern regions with a compensation factor for unevenness, and certain but definite control of lithographic tool moving speed.

However, after developing and etching, a sharp corner on the pattern never remains as it was. A compensatory lithographic tool trajectory for pattern deformation due to developing and etching should be kept in mind. Thus, these

make-ups need to be devised carefully in conjunction with the analysis of the experimental results upon developing and etching.

| N | Fig.2(a)    | Fig.2(b)    | Fig.2(c)    | Fig.2(d)    | Fig.2(e)    | Fig.2(f)    |
|---|-------------|-------------|-------------|-------------|-------------|-------------|
| 1 | 0.59        | 0.47        | 0.37        | 0.32        | 0.25        | 0.21        |
| 2 | <b>1.01</b> | 1.00        | 1.00        | 1.00        | 1.00        | 1.00        |
| 3 | 1.02        | <b>1.00</b> | 0.99        | 0.97        | 0.91        | 0.88        |
| 4 | 1.02        | 1.00        | <b>1.00</b> | 1.00        | 1.00        | 1.00        |
| 5 | 1.02        | 1.00        | 1.00        | <b>1.00</b> | 1.00        | 0.99        |
| 6 | 1.03        | 1.00        | 1.00        | 1.00        | <b>1.00</b> | 1.00        |
| 7 | 1.03        | 1.01        | 1.00        | 1.00        | 1.00        | <b>1.00</b> |

Tab. 1. Half line thickness obtained at 50% of the maximum exposure intensity.

### 3. GENERATION OF LITHOGRAPHIC TOOL PATH

In pocket machining fields, the efficient path is told as the path with minimal tool retraction and no over milling. In lithography fields, the efficient lithographic path may be similar to that in pocket machining. Thus, reconsideration on over milling and tool retraction in the view of energy accumulation and isolation is inevitable.

Over milling in direct write lithography means over traversal along the path. One time over milling causes a double increase of the irradiance. It surely results in marking on the lithography product due to uneven exposure, if it is 200%. Thus, a lithographic tool path generation method must be free from over traversal.

Tool retraction in direct write lithography means either over exposure along the retractive path or the beam being turned off while in retraction which is time consuming. Thus, tool retraction should be minimized if there exist any separated regions and it must be avoided within the whole extent of the continuous region.

To enable the method to be applied for various lithographic patterns, the method should possess both robustness and flexibility. To be welcomed by lithography equipment manufacturers, the method must generally but accurately find a lithographic path upon any requirement by the customer such as the starting position or the ending position of the lithographic path.

In this section, the detail of the lithographic tool path generation process is discussed, through an illustrative example of pocketing, using the Offset Loop Entity (OLE) and Path link Entity (PE) concepts, following the Offset-loop Dissection Method (ODM) and Path Determination Method (PDM) by Seo et. al. [7]. The PDM based on the OLE/PE concepts is so simple that the determination of the linking sequence is accomplished by two searches; 1) the Breadth First Search (BFS) on the OLE Generation History (OGH) graph and 2) the Depth First Search (DFS) on the Tool Path (TP) tree. Even so, the method is robust and flexible enough to generate a lithographic path for minimized beam retraction and over traversal free lithography under any kind of pattern geometry or equipment configuration.

An illustrated example of the OLE map generated by ODM algorithm [7] for a pocket with two islands is shown in Fig. 3(a). As the first step, the OGH graph is constructed by connecting valid OLEs during offsetting as shown in Fig. 3(b). By means of the OGH graph, the OLE is stored in a linked list data structure such that the lineage of OLE is expressed as a tree data structure. The information about the relationships among OLEs through the successive offsetting is contained in the OGH graph. The OLE itself is represented as a node and the birth of OLE is expressed using branches like a family tree.

For this specific example, 28 valid OLEs are connected with 30 branches in the sequence of generation throughout offsetting. However, anyone looking at the graph could find that the minimal number of branches needed to connect 28 OLEs is 27. Over traversal is unavoidable if all 30 branches in Fig. 3(b) are selected as the linking path segments for 28 OLEs. Thus, the modification of the OGH graph is inevitable to discard the redundant branches responsible for over traversal.

The OLE where the lithography starts is selected as the second step by considering technological constraints, such as beam retraction and/or beam off. From the selected starting OLE, the BFS on the undirected OGH graph is performed.

Then, the TP tree is constructed upon the BFS result by linking all OLEs with the minimal number of PEs instead of excessive branches as shown in Fig. 3(c).

The relational information about the OLEs/PEs with linking sequence and the geometric information on the OLEs are contained in the TP tree. The OLE<sub>28</sub> is selected as a starting OLE for outward writing. The result shows that the reduction on the number of over traversal is accomplished by the BFS search.

By linking all OLEs with the minimal number of PEs in Fig. 3(c), three redundant branches (b<sub>12</sub>, b<sub>13</sub>, b<sub>14</sub>) from Fig. 3(b) are discarded. Although the TP tree contains additional information on PEs, it is still not possible to start on actual writing relying only upon the information contained in the TP tree. Therefore, the geometric information on the PEs such as its position and entry/exit point must be determined.

The OLE where the writing ends is selected as the third step by considering technological constraints and by accounting the number of PEs to the starting OLE. The one-way path from the starting OLE to the ending OLE is set. The PEs in the one-way path are placed onto the OLE map with the location of an entry/exit point on the OLE. The OLEs/PEs in the one-way path are marked on the TP tree.

Forming the shortest line segment upon upper PE position, the rest of PEs in breadth of the marked path are placed onto the OLE map in the breadth order with the location of an entry/exit point on the OLE. As the result of the PE placement on the OLE map, the parental OLE having two and more successive OLEs in the TP tree appears with multiple entry/exit points on it. The consideration on the visiting sequence of multiple entry/exit points existing on a single OLE is left for the next step.

In this specific example, the OLE<sub>1</sub> is selected as an ending OLE. The PEs (PE<sub>30</sub>, PE<sub>26</sub>, PE<sub>21</sub>, PE<sub>16</sub>, PE<sub>7</sub>, PE<sub>4</sub>, PE<sub>1</sub>) in the one-way path are placed onto the OLE map with the bold lined arrow as shown in Fig. 3(d). The OLEs (OLE<sub>28</sub>, OLE<sub>24</sub>, OLE<sub>19</sub>, OLE<sub>14</sub>, OLE<sub>9</sub>, OLE<sub>7</sub>, OLE<sub>4</sub>, OLE<sub>1</sub>) and the PEs in the one-way path are marked on the TP tree to be searched last. Then, the rest of PEs in breadth of the marked path are placed onto the OLE map with the thin lines having the location of an entry/exit point as shown in Fig. 3(d).

The possibility of over traversal is not negligible, since the parental OLEs having two and more successive OLEs showed up with multiple entry/exit points on them shown as OLE<sub>19</sub>, OLE<sub>9</sub>, OLE<sub>7</sub>, OLE<sub>11</sub>, OLE<sub>15</sub> in Fig. 3(c), Fig. 3(d) and Fig. 3(e). Therefore, the visiting sequence of multiple entry/exit points should be ordered properly.

The OLEs/PEs in the marked path are placed on the rightmost of the TP tree to be searched last as the fourth step. The OLEs/PEs in breadth of the marked path are reordered comparing the travel distance upon parental OLE orientation for visiting sequence. In Fig. 3(e), the bold lined marked path being planned to be searched last OLE<sub>28</sub> → OLE<sub>24</sub> → OLE<sub>19</sub> → OLE<sub>14</sub> → OLE<sub>9</sub> → OLE<sub>7</sub> → OLE<sub>4</sub> → OLE<sub>1</sub> is shown on the rightmost side.

To prevent over traversal, the breadth order OLE<sub>13</sub> → OLE<sub>7</sub> → OLE<sub>8</sub> is changed to OLE<sub>13</sub> → OLE<sub>8</sub> → OLE<sub>7</sub> considering the counterclockwise orientation of parental OLE (OLE<sub>9</sub>), and the breadth order OLE<sub>4</sub> → OLE<sub>5</sub> → OLE<sub>10</sub> → OLE<sub>11</sub> → OLE<sub>12</sub> is changed to OLE<sub>12</sub> → OLE<sub>11</sub> → OLE<sub>10</sub> → OLE<sub>5</sub> → OLE<sub>4</sub> considering the counterclockwise orientation of parental OLE (OLE<sub>7</sub>) as shown in Fig. 3(c), Fig 3(d), and Fig. 3(e).

The DFS on the arranged TP tree is performed as the last step. To avoid beam retractions, the marked one-way path is searched last. The shortest path upon the DFS result is written down and saved as the lithographic path without beam over traversal and beam retraction.

As discussed, the selection of a starting point or an ending point of lithography is not restricted at all. Regardless of the starting/ending point, the method generates the shortest path from the starting point to the ending point. By being able to freely select a starting point or an ending point of lithography path, the design or operation of the lithography equipment may become easier.

On the other hand, the selection of starting and ending points is crucial for the reduction of the travel distance of the beam. The proposed method enables the efficient selection of starting and ending points feasible. Upon the selection of the starting/ending point, the total length of the most efficient path,  $L$ , may be written as:

$$L = \sum_{i=1}^n l_i + d(2n - m - 1) \quad (3)$$

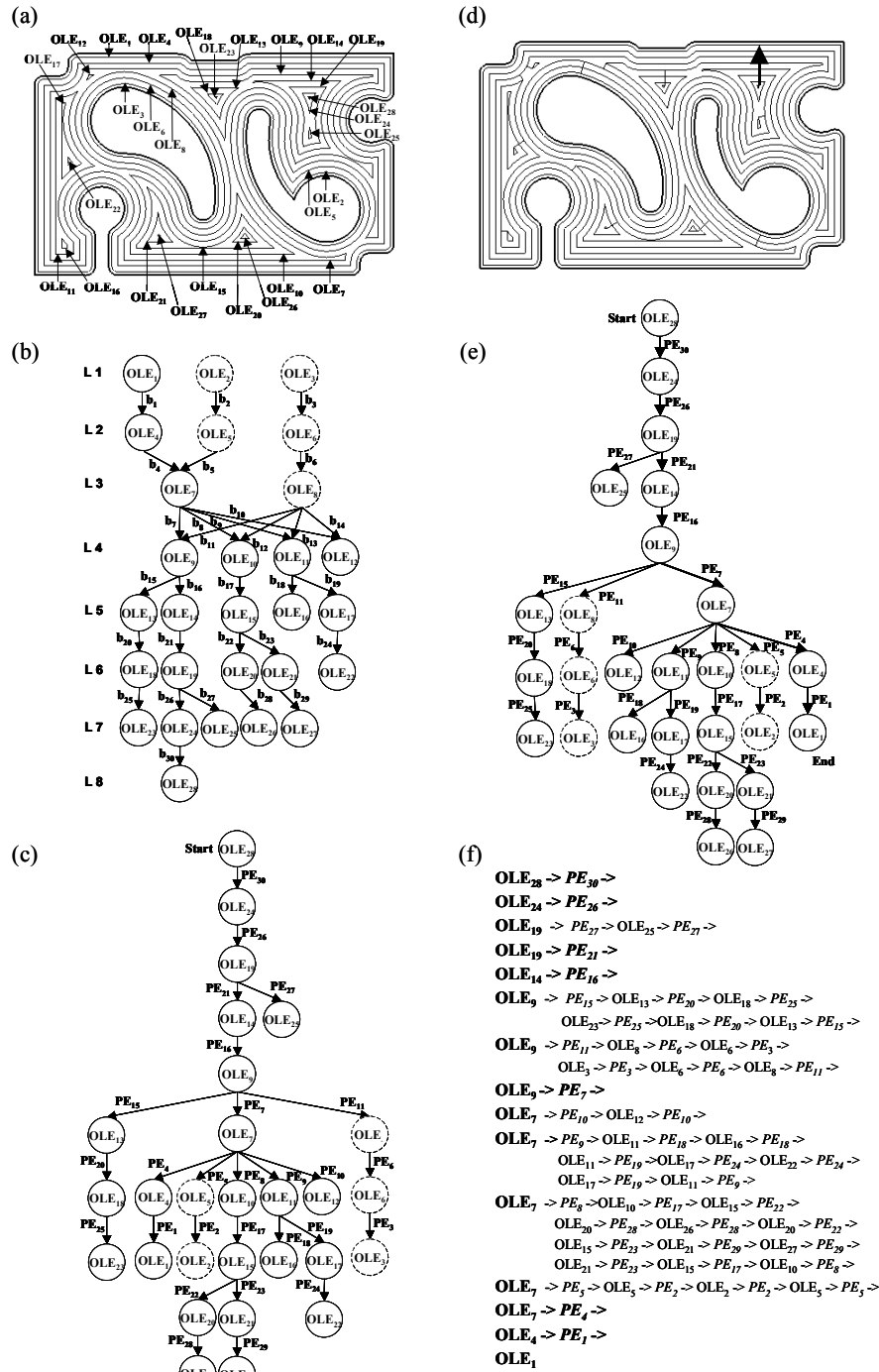


Fig. 3. Lithographic tool path generation process.

where,  $n$  is the total number of OLEs,  $l_i$  is the length of the OLE  $i$ ,  $d$  is the fixed offset distance, and  $m$  is the number of OLEs on the main path. By increasing  $m$  in Eqn. 3, the total distance for lithographic tool to travel,  $L$ , is

reduced. Thus, we may say that the method optimizes the lithographic path to be the most efficient one upon the selection of the starting/ending point. Therefore, the optimal lithographic path enables speedy lithography.

#### 4. RESULTS AND DISCUSSION

In order to verify the robustness of the proposed lithographic path generation method, a prototype system is implemented using C language and OpenGL graphic library. The implemented system is then examined using the barrier rib of the RGB pattern, the Printed Circuit Board(PCB) pattern, and the Indium Tin Oxide (ITO) pattern.

The screen images of the lithographic path obtained from the implemented system are shown in Fig. 4, Fig. 5 and Fig. 6. The portion of barrier rib of the RGB pattern exposed on its negative side is shown in Fig. 4, the PCB pattern exposed on its negative side is shown in Fig. 5, and the portion of the ITO pattern and its two enlarged portions exposed on its positive side are shown in Fig. 6. The results verify that the devised lithographic path generation method is concise and simple, but robust and flexible enough to generate a lithographic path under constraints such as exposure intensity accumulation, and even enough to generate the optimal lithographic path for speedy lithography.

#### 5. CONCLUSION

Through this study, it is confirmed that the adoption of the offset curve generation method and tool path generation method into lithographic path generation for direct write lithography is proper and reliable. The accuracy of the method is ensured by the uniformity of the irradiance. The efficiency of the method is increased upon the shortening of the lithographic path. Moreover, the burdensome and time consuming control of on/off for a laser beam in conventional direct write lithography is minimized in the method.

Future study will be concentrated on the development of a method to compensate for the deviation from the flattened irradiance due to lithographic pattern geometries, lithographic speed variations, and lithography conditions such as developing and/or etching in conjunction with the analysis of the experimental results upon developing and etching.

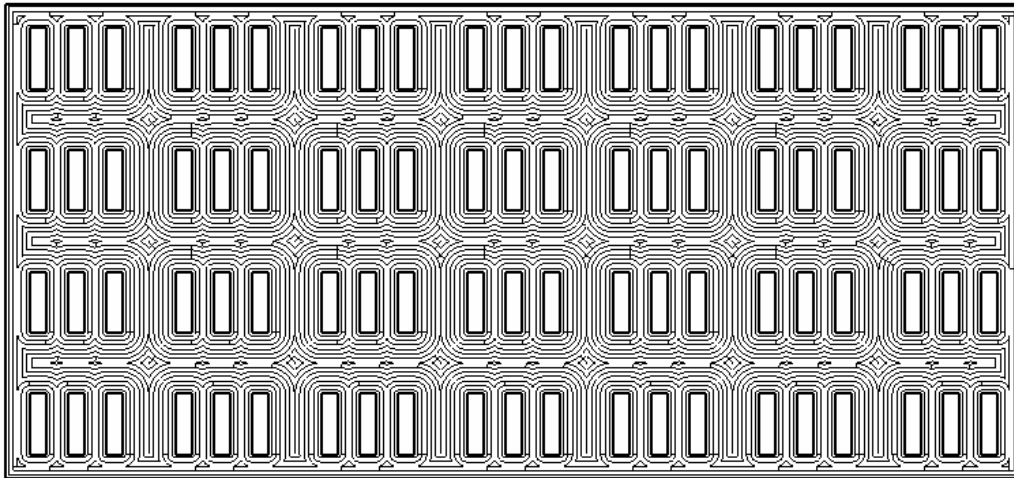


Fig. 4. The lithographic path for the portion of barrier rib of RGB pattern.

#### 6. REFERENCES

- [1] Beeker, A., Cebuhar, W., Kreuzer, J., Latypov, A., and Vladimisky, Y., Methods and Systems to compensate for a stitching disturbance of a printed pattern in a maskless lithography system utilizing overlap of exposure zones with attenuation of the aerial image in the overlap region, *U.S. Patent No.6,876,440 B1*, 2005.
- [2] Chan, K. F., Feng, Z., Yang, R., Ishikawa, A., and Mei, W., High-resolution maskless lithography, *Journal of Microlithography, Microfabrication, and Microsystems*, Vol. 2, No. 4, 2003, pp 331-339.
- [3] Seo, M. and Kim, H., Occupancy based pattern generation method for maskless lithography, *Patent pending in Korea, Application Pub. No.10-2005-0114003*, 2005

- [4] Spence, C., Tabery, Y., Cantrall, R., Dahl, L., Buck, P., and Wilkinson, B., A comparison of DUV wafer and reticle Lithography – What is the limit?, *22<sup>nd</sup> Annual BACUS symposium on photomask Technology, Proceedings of SPIE*, Vol.4889, 2002, pp177-186.
- [5] Blumenstock, G. M., Duffey, T. P., Onkels, E. and Sandstrom, R., F2(157nm) laser for VUV microlithography, *SEMI Technology Symposium*, 1999, p 99.
- [6] Swencen, E., Sun, Y. and Dunsky, C., Laser micromachining in electronics manufacturing: A historical Overview, *Proceedings of SPIE*, Vol. 4095, 2000.
- [7] Seo, M., Kim, H., and Onosato, M., Systematic approach to contour-parallel tool path generation of 2.5-D pocket with islands, *Computer-Aided Design and Applications*, Vol. 2, Nos. 1-4, 2005, pp 213-222.

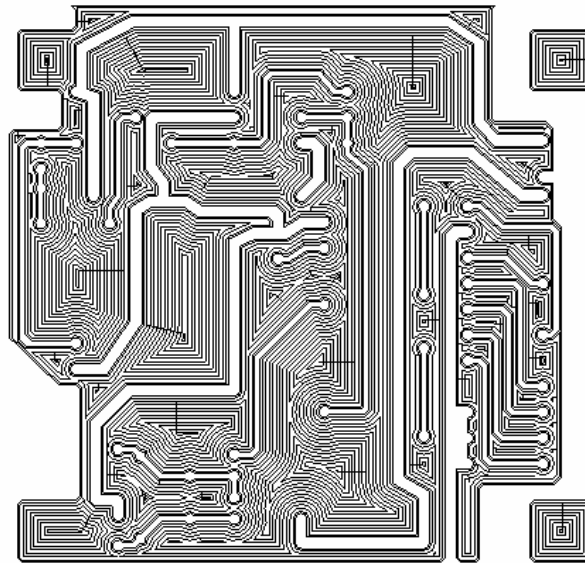


Fig. 5. The lithographic path for the PCB pattern.

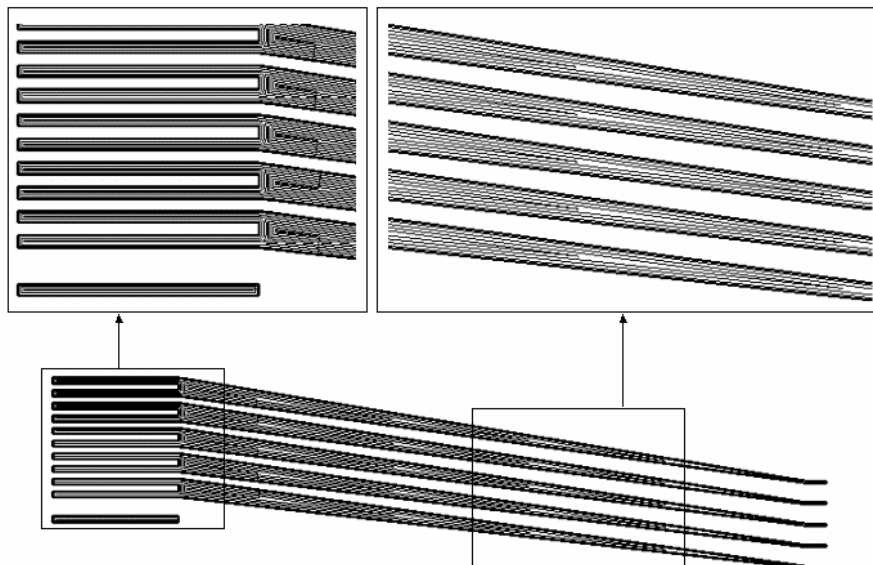


Fig. 6. The lithographic path for the portion of ITO pattern.